Inorg. Chem. **2003**, *42*, 1508–1517

Oxovanadium(IV) and -(V) Complexes of Dithiocarbazate-Based Tridentate Schiff Base Ligands: Syntheses, Structure, and Photochemical Reactivity of Compounds Involving Imidazole Derivatives as Coligands

Satyabrata Samanta,[†] Dipesh Ghosh,[†] Suman Mukhopadhyay,[†] Akira Endo,[‡] Timothy J. R. Weakley,[§] and Muktimoy Chaudhury*[,†]

Department of Inorganic Chemistry, Indian Association for the Cultivation of Science, Kolkata 700 032, India, Department of Chemistry, Faculty of Science and Technology, Sophia University, 7-1 Kioi-cho, Chiyoda-ku, Tokyo 102-8554, Japan, and Department of Chemistry, University of Oregon, Eugene, Oregon 97403

Received July 8, 2002

The tridentate dithiocarbazate-based Schiff base ligands H_2L (*S*-methyl-3-((5-R-2-hydroxyphenyl)methyl)dithiocarbazate, R = NO_2, L = L^2; R = Br, L = L^3) react with $[VO(acac)_2]$ in the presence of imidazole derivatives as coligands to form oxovanadium(IV) and *cis*-dioxovanadium(V) complexes. With benzimidazole and *N*-methylimidazole, the products are oxovanadium(IV) complexes, viz. $[VOL^3(BzIm)]\cdot 0.5CH_3CN$ (**1a**) and $[VOL(N\text{-MeIm})_2]$ (L = L^3, **1b**; L = L^2, **1c**), respectively. In both **1a**,**b**, the O and S donor atoms of the tridentate ligand are cis to the terminal oxo group (in the "equatorial" plane) and mutually trans, but the N donor atom is respectively cis and trans to the oxo atom, as revealed from X-ray crystallography. When imidazole or 4-methylimidazole is used as the ancillary ligand, the products obtained are water-soluble *cis*-dioxovanadium(V) complexes $[VO_2L(R'\text{-ImH})]$ (L = L^3 and L^2, R′ = H and Me, **2a**–**d**). These compounds have zigzag chain structures in the solid state as confirmed by X-ray crystallographic investigations of **2a**,**d**, involving an alternating array of LVO_2^- species and the imidazolium counterions held together by Coulombic interactions and strong hydrogen bonding. Complexes **2a**–**d** are stable in water or methanol. In aprotic solvents, viz. CH_3CN, DMF, or DMSO, however, they undergo photochemical transformation when exposed to visible light. The putative product is a mixed-oxidation divanadium(IV/V) species obtained by photoinduced reduction as established by EPR, electronic spectroscopy, and dynamic ^1H NMR experiments.

Introduction

The identities of vanadium biochromophores in haloperoxidase enzymes have been under close scrutiny by various spectroscopic investigations.[1−10] Many of these studies have indicated the presence of imidazole moiety (histidine) in the vanadium active sites of these enzymes. In aqueous solutions, the equilibrium and kinetics studies of many vanadate reactions are found to be significantly altered by the presence of imidazole in the reaction media.[11,12] Also many phosphorylase enzymes are known to contain histidine residues that

* To whom correspondence should be addressed. E-mail: icmc@mahendra.iacs.res.in.
[†] Indian Association for the Cultivation of Science.
[‡] Sophia University.
[§] University of Oregon.

(1) (a) *Vanadium in Biological Systems*; Chasteen, N. D., Ed.; Kluwer Academic Publishers: Dordrecht, The Netherlands, 1990. (b) Butler, A.; Carrano, C. J. *Coord. Chem. Rev.* **1991**, *109*, 61. (c) Rehder, D. *Angew. Chem., Int. Ed. Engl.* **1991**, *30*, 148.
(2) Rehder, D.; Holst, H.; Priebsch, W.; Vilter, H. *J. Inorg. Biochem.* **1991**, *41*, 171.
(3) Arber, J. M.; de Boer, E.; Garner, C. D.; Hasnain, S. S.; Wever, R. *Biochemistry* **1989**, *28*, 7968.
(4) Rehder, D.; Vilter, H.; Duch, A.; Priebsch, W.; Weidemann, C. *Recl. Trav. Chim. Pays-Bas* **1987**, *106*, 408.
(5) de Boer, E.; Boon, K.; Wever, R. *Biochemistry* **1988**, *27*, 1629.
(6) Chasteen, N. D. In *Biological Magnetic Resonance*; Berliner, L. J., Reuben, J., Eds.; Plenum Press: New York, 1981; Vol. 3, pp 53−119.
(7) de Boer, E.; Keijzers, C. P.; Klaassen, A. A. K.; Reijerse, E. J.; Collison, D.; Garner, C. D.; Wever, R. *FEBS Lett.* **1988**, *235*, 93.
(8) de la Rosa, R. I.; Clague, M. J.; Butler, A. *J. Am. Chem. Soc.* **1992**, *114*, 760.
(9) Colpas, G. J.; Hamstra, B. J.; Kampf, J. W.; Pecoraro, V. L. *J. Am. Chem. Soc.* **1994**, *116*, 3627.
(10) Messerschmidt, A.; Wever, R. *Proc. Natl. Acad. Sci. U.S.A.* **1996**, *93*, 392.
(11) Vyskocil, F.; Teisinger, J.; Dlouha, H. *Nature* **1980**, *286*, 516.
(12) Crans, D. C.; Schelble, S. M.; Theisen, L. A. *J. Org. Chem.* **1991**, *56*, 1266.

10.1021/ic020438v CCC: $25.00
Published on Web 02/12/2003

coordinate to vanadium center.[13] All these have generated sufficient interest in recent times to understand the coordination chemistry of vanadium in biologically relevant ligand environments involving imidazole as donor.[14−18]

Over the past few years we have been working on the coordination chemistry of oxovanadium species, using sulfur containing tri- and tetradentate ligands.[19−23] The use of tridentate ligands in oxometalate chemistry has an intrinsic advantage because of their ability to form the MOL primary core, leaving open at least one or more coordination site(s) for the acceptance of ancillary ligands to complete the coordination geometry.[24,25] We have exploited these coordination possibilities for the syntheses of structurally and kinetically interesting mono-, bi-, and polynuclear oxovanadium complexes using dithiocarbazate-based Schiff base molecules (H_2L, L = L^1−L^3) as tridentate ligands.[19,20,22,23]

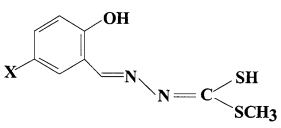

H_2L

X	H_2L
H	H_2L^1
NO_2	H_2L^2
Br	H_2L^3

Herein, we report the syntheses of oxovanadium(IV) and -(V) complexes of the aforesaid tridentate ligands in the presence of various imidazole derivatives as coligands. Electronic and molecular structures of these compounds have been examined in details. Photochemical reduction of the *cis*-dioxovanadium(V) complexes into mixed-oxidation divanadium(IV/V) products is also established.

Experimental Section

Materials. The tridentate ligands (H_2L^2 and H_2L^3)[26,27] and the precursor complex $[VO(acac)_2]$[28] were prepared by following the reported methods. Reagent grade solvents were dried from appropriate reagents[29] and distilled under nitrogen prior to their use. All other chemicals were commercially available and used as received.

Preparation of Complexes. $[VOL^3(BzIm)]\cdot 0.5CH_3CN$ (1a). To an acetonitrile solution (15 mL) of $[VO(acac)_2]$ (0.27 g, 1 mmol) was added 0.31 g of the ligand H_2L^3 (1 mmol) in 10 mL of the same solvent. It was refluxed for 15 min to get a brown solution. To this was then added an aqueous solution (15 mL) of benzimidazole (0.14 g, 1.2 mmol), and the resulting mixture was further refluxed for an additional 2 h when a deep green solution was obtained. It was filtered and cooled at 0 °C for an overnight period when a green microcrystalline product was deposited. The compound was collected by filtration, washed with diethyl ether (4 × 10 mL), and finally dried in vacuo. The product was recrystallized from acetonitrile solvent. Yield: 0.22 g (44%). Anal. Calcd for $C_{17}H_{14.5}BrN_{4.5}O_2S_2V$: C, 40.11; H, 2.85; N, 12.38. Found: C, 39.9; H, 2.8; N, 12.2. IR (KBr disk, cm^{-1}): ν(C⋯N), 1598 s; ν(C⋯O/phenolate), 1528 s; ν(V═O_t), 960 s.

$[VOL^3(N\text{-}MeIm)_2]$ (1b). A solution of $[VO(acac)_2]$ (0.27 g, 1 mmol) in acetonitrile (20 mL) was added to an equimolar amount of the ligand H_2L^3 (0.31 g, 1 mmol) taken in the same solvent (15 mL) and refluxed for 10 min. To the resulting brown solution was added an aqueous solution (10 mL) of *N*-methylimidazole (0.18 g, 2.2 mmol), and the resulting solution was heated again at reflux temperature for ca. 4 h to get a clear brown solution. It was filtered, and the filtrate volume was reduced to ca. 20 mL by rotary evaporation and finally cooled in a freezer at 0 °C for an overnight period. A brown crystalline compound that deposited at this stage was collected by filtration, washed with diethyl ether (4 × 10 mL), and dried in vacuo. The product was recrystallized from acetonitrile solvent. Yield: 0.26 g (48%). Anal. Calcd for $C_{17}H_{19}BrN_6O_2S_2V$: C, 38.20; H, 3.56; N, 15.73. Found: C, 37.6; H, 3.6; N, 15.2. IR (KBr disk, cm^{-1}): ν(C⋯N), 1592 s; ν(C⋯O/phenolate), 1536 s; ν(V═O_t), 954 s.

$[VOL^2(N\text{-}MeIm)_2]$ (1c). This compound was prepared by following essentially the same procedure as described above for **1b** using H_2L^2 as the tridentate ligand. The brown crystalline product was obtained in 54% yield. Anal. Calcd for $C_{17}H_{19}N_7O_4S_2V$: C, 40.80; H, 3.80; N, 19.60. Found: C, 41.1; H, 3.7; N, 19.3. IR (KBr disk, cm^{-1}): ν(C⋯N), 1595 s; ν(C⋯O/phenolate), 1537 s; ν(V═O_t), 951 s.

$[VO_2L^3(ImH)]_\infty$ (2a). To a solution of $[VO(acac)_2]$ (0.27 g, 1 mmol) in acetonitrile (15 mL) was added stoichiometric amount (1:1 mole ratio) of the ligand H_2L^3 (0.31 g), also taken in the same solvent (15 mL). The solution was refluxed for 10 min and then cooled to room temperature to get a brown solution. To this was then added an aqueous solution (7 mL) of imidazole (0.08 g, 1.18 mmol), and the resulting mixture was further refluxed for 1 h. The resulting green solution obtained at this stage was filtered and kept in the air for several days becoming gradually yellow in color. It was filtered, the filtrate volume was reduced to ca. 15 mL by rotary

(13) Lindqvist, Y.; Schneider, G.; Vihko, P. *Eur. J. Biochem.* **1994**, *221*, 139.
(14) Cornmann, C. R.; Kampf, J.; Pecoraro, V. L. *Inorg. Chem.* **1992**, *31*, 1981.
(15) Cornmann, C. R.; Kampf, J.; Lah, M. S.; Pecoraro, V. L. *Inorg. Chem.* **1992**, *31*, 2035.
(16) Calviou, L. J.; Arber, J. M.; Collison, D.; Garner, C. D.; Clegg, W. *J. Chem. Soc., Chem. Commun.* **1992**, 654.
(17) Keramidas, A. D.; Miller, S. M.; Anderson, O. P.; Crans, D. C. *J. Am. Chem. Soc.* **1997**, *119*, 8901.
(18) Crans, D. C.; Keramidas, A. D.; Hoover-Litty, H.; Anderson, O. P.; Miller, M. M.; Lemoine, L. M.; Pleasic-Williams, S.; Vandenberg, M.; Rossomando, A. J.; Sweet, L. J. *J. Am. Chem. Soc.* **1997**, *119*, 5447.
(19) Dutta, S. K.; Kumar, S. B.; Bhattacharyya, S.; Tiekink, E. R. T.; Chaudhury, M. *Inorg. Chem.* **1997**, *36*, 4954.
(20) Dutta, S. K.; Samanta, S.; Kumar, S. B.; Han, O. H.; Burckel, P.; Pinkerton, A. A.; Chaudhury, M. *Inorg. Chem.* **1999**, *38*, 1982.
(21) Bhattacharyya, S.; Mukhopadhyay, S.; Samanta, S.; Weakley, T. J. R.; Chaudhury, M. *Inorg. Chem.* **2002**, *41*, 2433.
(22) Dutta, S. K.; Samanta, S.; Mukhopadhyay, S.; Burckel, P.; Pinkerton, A. A.; Chaudhury, M. *Inorg. Chem.* **2002**, *41*, 2946.
(23) Dutta, S. K.; Samanta, S.; Ghosh, D.; Butcher, R. J.; Chaudhury, M. *Inorg. Chem.* **2002**, *41*, 5555.
(24) Craig, J. A.; Harlan, E. W.; Snyder, B. S.; Whitener, M. A.; Holm, R. H. *Inorg. Chem.* **1989**, *28*, 2082.
(25) Topich, J.; Lyon, J. T., III. *Inorg. Chem.* **1984**, *23*, 3202.
(26) Dutta, S. K.; Tiekink, E. R. T.; Chaudhury, M. *Polyhedron* **1997**, *16*, 1863.
(27) Abbreviations used: H_2L^1, *S*-methyl-3-((2-hydroxyphenyl)methyl)-dithiocarbazate; H_2L^2, *S*-methyl-3-((5-nitro-2-hydroxyphenyl)methyl)-dithiocarbazate; H_2L^3, *S*-methyl-3-((5-bromo-2-hydroxyphenyl)methyl)-dithiocarbazate; Hacac, acetylacetone; Im, imidazole; BzIm, benzimidazole; *N*-MeIm, *N*-methylimidazole; TEAP, tetraethylammonium perchlorate.
(28) Rowe, R. A.; Jones, M. M. *Inorg. Synth.* **1957**, *5*, 113.
(29) Perrin, D. D.; Armarego, W. L. F.; Perrin, D. R. *Purification of Laboratory Chemicals*, 2nd ed.; Pergamon: Oxford, England, 1980.

Table 1. Relevant Crystal Data for $[VOL^3(BzIm)]\cdot 0.5CH_3CN$ (**1a**), $[VOL^3(N\text{-}MeIm)_2]$ (**1b**), $[VO_2L^3(ImH)]_\infty$ (**2a**), and $[VO_2L^2(4\text{-}MeImH)]_\infty$ (**2d**)

	1a	1b	2a	2d
composn	$C_{17}H_{14.5}BrN_{4.5}O_2S_2V$	$C_{17}H_{19}BrN_6O_2S_2V$	$C_{12}H_{12}BrN_4O_3S_2V$	$C_{13}H_{14}N_5O_5S_2V$
fw	508.8	534.3	455.22	435.4
space group	orthorhombic $P2_12_12$ (No. 18)	monoclinic $P2_1/c$ (No. 14)	monoclinic $P2_1/a$ (No. 14)	monoclinic $C2/c$ (No. 15)
a, Å	15.4564(11)	9.1958(18)	6.6680(3)	22.401(4)
b, Å	31.732(2)	20.970(7)	13.968(2)	12.650(3)
c, Å	8.3310(2)	12.1575(27)	18.441(3)	13.836(9)
β, deg		111.51(2)	93.30(3)	115.48(4)
V, Å^3	4085.9(7)	2181(1)	1714(1)	3539(3)
Z	8	4	4	8
ρ_{calcd}, g cm^{-3}	1.654	1.627	1.764	1.634
T, °C	23	22	22	23
λ, Å	0.710 73	0.710 73	0.710 73	0.710 73
μ, cm^{-1}	26.7	25.1	31.2	8.32
rel transm coeff(ψ scans)	0.795−1.000	0.670−1.000	0.675−1.000	0.89−1.00
no. obsd reflcns [$I \geq \sigma(I)$]	2438	2493	2090	2465
tot. indepdt reflcns	4050	3725	2996	3115
R(F), wR(F) (obsd data)[a]	0.059, 0.052	0.058, 0.046	0.055, 0.057	0.041, 0.042
R(F^2), wR(F^2) (all data)[a]	0.102, 0.105	0.084, 0.094	0.091, 0.110	0.063, 0.085

[a] $R = \sum||F_o| - |F_c||/\sum|F_o|$; $wR(F^2) = [\sum w(|F_o|^2 - |F_c|^2)^2/\sum w|F_o|^4]^{1/2}$.

evaporation, and finally cooled in a refrigerator at 4 °C for an overnight period to get a yellow crystalline product. It was collected by filtration, washed with diethyl ether, and finally recrystallized from methanol/water (3:1 v/v) mixture. Yield: 0.27 g (60%). Anal. Calcd for $C_{12}H_{12}BrN_4O_3S_2V$: C, 31.65; H, 2.64; N, 12.31. Found: C, 32.2; H, 2.6; N, 12.2. IR (KBr disk, cm^{-1}): ν(C⋯N), 1592 s; ν(C⋯O/phenolate), 1537 s; ν(V═O$_t$) 932 s, 835 s.

$[VO_2L^2(ImH)]_\infty$ (2b). This complex was prepared from $[VO(acac)_2]$ (0.27 g, 1 mmol), ligand H_2L^2 (0.27 g, 1 mmol), and imidazole (0.08 g, 1.18 mmol) using the methodology analogous to that described above for **2a**. Yield: 54%. Anal. Calcd for $C_{12}H_{12}N_5O_5S_2V$: C, 34.20; H, 2.85; N, 16.63. Found: C, 34.3; H, 2.9; N, 17.0. IR (KBr disk, cm^{-1}): ν(C⋯N), 1605 s; ν(C⋯O/phenolate), 1533 s; ν(V═O$_t$), 958 s, 842 s.

$[VO_2L^3(4\text{-}MeImH)]_\infty$ (2c). This compound was synthesized using a similar method as employed for **2a** by using 4-methylimidazole instead of imidazole. Yield: 49%. Anal. Calcd for $C_{13}H_{14}BrN_4O_3S_2V$: C, 33.26; H, 2.98; N, 11.94. Found: C, 33.5; H, 3.0; N, 12.0. IR (KBr disk, cm^{-1}): ν(C⋯N), 1598 s; ν(C⋯O/phenolate), 1536 s; ν(V═O$_t$), 915 s, 820 s.

$[VO_2L^2(4\text{-}MeImH)]_\infty$ (2d). This compound was obtained in 51% yield by following the same procedure as for **2a** but using H_2L^2 and 4-methylimidazole as the ligands. Anal. Calcd for $C_{13}H_{14}N_5O_5S_2V$: C, 35.86; H, 3.22; N, 16.09. Found: C, 36.1; H, 3.3; N, 16.2. IR (KBr disk, cm^{-1}): ν(C−N), 1600 s; ν(C−O/phenolate), 1553 s; ν(V═O$_t$), 953 s, 833 s.

Physical Measurements. Details of elemental (C, H, and N) analyses and IR and UV−vis spectral measurements were described elsewhere.[20,30] The ^{1}H NMR spectra were recorded on a Bruker model Avance DPX 300 spectrometer. Magnetic moments of the powdered polycrystalline samples at room temperature were calculated from the data obtained on a PAR 155 vibrating-sample magnetometer. X-band EPR spectra in solution at room temperature and in the frozen state (77 K) were recorded on a Bruker model ESP 300 E spectrometer equipped with standard Bruker attachments and also on a JES-3X spectrometer equipped with a JEOL ES-PRIT 330 data processing system. Cyclic voltammetric measurements were performed on a PAR electrochemical analyzer (model 250/5/0) in dry acetonitrile under purified dinitrogen with TEAP as the supporting electrolyte. A glassy carbon working, a platinum wire counter and saturated calomel reference (SCE) electrodes were used for these measurements. The ferrocenium/ferrocene (Fc^+/Fc) couple was used as the internal standard.

X-ray Crystallography. Diffraction-quality crystals of $[VOL^3(BzIm)]\cdot 0.5CH_3CN$ (**1a**) (green prism, 0.05 × 0.14 × 0.47 mm obtained from CH_3CN solution), $[VOL^3(N\text{-}MeIm)_2]$ (**1b**) (dark red-brown tablet, 0.21 × 0.41 × 0.43 mm obtained from CH_3CN/CH_3OH (1:1 v/v) mixture), $[VO_2L^3(ImH)]_\infty$ (**2a**) (yellow plate, 0.05 × 0.36 × 0.58 mm obtained from CH_3OH/H_2O mixture), and $[VO_2L^2(4\text{-}MeImH)]_\infty$ (**2d**) (amber prism, 0.20 × 0.23 × 0.43 mm obtained from CH_3CN/CH_3OH (1:1 v/v) solution)) were obtained from the designated solvents by slow evaporation. The orientation parameters and cell dimensions were obtained from the setting angles of an Enraf-Nonius CAD-4 diffractometer fitted with graphite-monochromatized Mo Kα radiation for 25 centered reflections in the range 13.2° ≤ θ ≤ 14.7°, 13.3° ≤ θ ≤ 14.9°, 12.9° ≤ θ ≤ 14.8°, and 12.2° ≤ θ ≤ 14.5° for **1a**, **1b**, **2a**, and **2d**, respectively. The crystal data and the final residuals are summarized in Table 1. Absorption corrections based on azimuthal scans ("ψ-scans") were applied.

For **1a**, the only systematic absences were: $hk0$, h odd, and $0k0$, k odd. The implied symmetry elements in turn required a glide plane normal to a, although there were no absences in the $0kl$ reflections. It was assumed that the $h00$ absences, but not the apparent $hk0$ absences, were genuine, i.e., that the space group was $P2_12_12$. A *SIR 92 E*-map[31] then showed all non-hydrogen atoms of two independent but very similar molecules with coordinates of the corresponding atoms related approximately as x, y, z and $0.5 + x, y, 0.40 - z$ (i.e. by a pseudo a glide normal to c). The C and N atoms of two independent CH_3CN molecules on crystal diad axes were refined isotropically. Their parameters had to be fixed in the last cycles to ensure convergence.

For **1b** and **2a**,**d**, the systematic absences together with the centric distribution of intensities indicated the space groups $P2_1/c$, $P2_1/a$, and $C2/c$, respectively. Absorption corrections based on azimuthal scans ("ψ-scans") were applied. A *SIR 92 E*-map[31] showed all the non- hydrogen atoms.

Hydrogen atoms were included at positions recalculated after each cycle of refinement [B(H) = 1.2B_{eq}(C); d(C−H) = 0.95 Å]. The final difference syntheses were featureless in all cases. The *TEXSAN* program suite[32] was used in all calculations.

(30) Bhattacharyya, S.; Weakley, T. J. R.; Chaudhury, M. *Inorg. Chem.* **1999**, *38*, 633.

(31) Altomare, A.; Cascarano, G.; Giacovazzo, C.; Burla, M. C.; Polidori, G.; Camalli, N. *J. Appl. Crystallogr.* **1994**, *24*, 435.

Scheme 1[a]

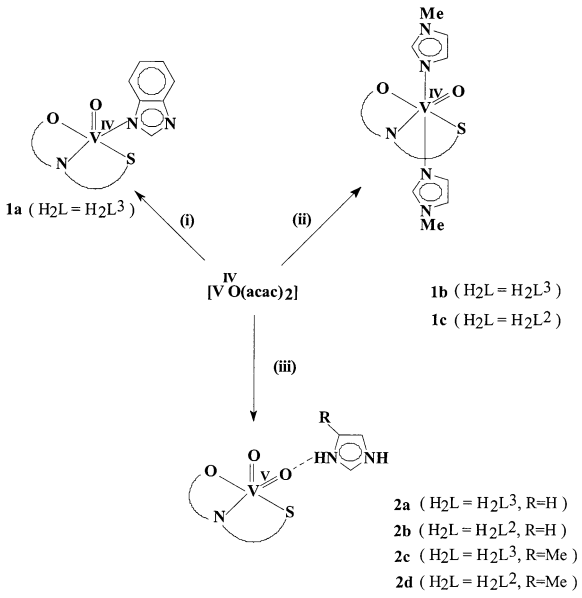

[a] Key: (i) 1:1:1 molar proportions of $[VO(acac)_2]$, H_2L^3, and benzimidazole; (ii) 1:1:2 molar proportions of $[VO(acac)_2]$, H_2L^2 (or H_2L^3), and *N*-methylimidazole; (iii) 1:1:1 molar proportions of $[VO(acac)_2]$, H_2L^2 (or H_2L^3), and imidazole (or 4-methylimidazole). All reactions were carried out in refluxing CH_3CN/H_2O mixture. In reaction iii, prolonged exposure to atmospheric oxygen is required to get the *cis*-dioxovanadium(V) products.

Photochemical Study. Clear yellow solutions of the complexes (**2a**−**d**) in CH_3CN were placed in quartz cell and purged with argon for 20 min. A tungsten filament lamp (60 W) was used as a visible light source to irradiate these solutions which gradually turned green with the passage of time during the photolysis. The green solutions obtained after different intervals of exposure time were used for subsequent characterization.

Results and Discussion

Syntheses. The synthetic strategy is outlined in Scheme 1. The oxovanadium(IV) complexes (**1a**−**c**) have been isolated as shining crystals, green to deep brown in color, in moderate yields (44−54%) by metathetical reactions involving stoichiometric amounts of $[VO(acac)_2]$, the tridentate ligand (H_2L^2 or H_2L^3), and the respective imidazole base (benzimidazole for **1a** and *N*-methylimidazole for **1b**,**c**) in acetonitrile/water medium at reflux temperature. When imidazole or 4-methylimidazole are used as the ancillary base, the green oxovanadium(IV) compounds that formed initially do not crystallize out because of their higher solubilities and undergo slow oxidation when allowed to stand in the air for several days. The products (**2a**−**d**) obtained are yellow crystalline solids with *cis*-dioxovanadium(V) center $[LVO_2(R'\text{-ImH})]_\infty$. The mandatory steps in the preparative procedure of **2a**−**d** are the presence of water in the reaction media and their subsequent exposure to atmospheric oxygen as confirmed by several control experiments. The products obtained are water-soluble compounds with zigzag chain structure and involve an alternating array of the anionic *cis*-dioxovanadium(V) $[LVO_2^-]$ species and the protonated imidazolium counterions, held together by strong Coulombic and hydrogen bonding interactions as revealed from X-ray crystallography (see later). A similar strategy of bonding interactions has been systematically utilized in crystal engineering to build up organic supramolecular architectures.[33]

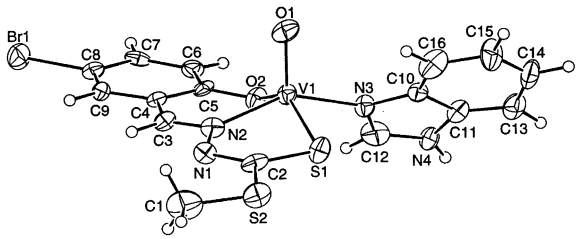

Figure 1. ORTEP diagram of $[VOL^3(BzIm)]\cdot 0.5CH_3CN$ (**1a**) with 30% thermal probability ellipsoids showing the atomic numbering scheme. CH_3CN is omitted for clarity.

Compound **1a,** when allowed to undergo aerial oxidation in aqueous acetonitrile medium, generated after ca. 1 week time a greenish yellow solution, from which we were unable to isolate the oxidized *cis*-dioxo product in analytically pure form. Both **1b**,**c,** on the other hand, are resistant to similar aerial oxidation under comparable experimental conditions. Thus, the basicity in the reaction medium, as influenced by the ancillary imidazole ligand, is a relevant factor in the oxidation to VO_2^+ species.[34]

IR spectra of the complexes are summarized in the Experimental Section. In each case, the spectrum displays the characteristic bands of the coordinated tridentate ligands.[19] In addition, a strong two-band pattern observed for **2a**−**d** in the 960−840 cm^{-1} region is the signature of the *cis*-dioxovanadium(V) moiety.[35] A single sharp band due to $V{=}O_t$ stretch is, however, observed at ca. 955 cm^{-1} for the vanadyl complexes (**1a**−**c**).

Description of Crystal Structures. Figures 1 and 2 display the perspective views of the vanadyl complexes **1a**,**b**, respectively. Their selected metrical parameters are given in Table 2. The asymmetric unit of **1a** contains two independent molecules; however, there are only minor conformational differences between them. The unit cell comprises eight molecules. The vanadium atom in each molecule is five-coordinate, existing in a distorted square pyramidal geometry in which the basal plane is defined by S(1), N(2), and O(2) atoms, derived from the tridentate ligand, and the N(3) atom from benzimidazole, the monodentate ancillary ligand. The apical position is occupied by the oxo atom O(1). The deviations from the least-squares plane through the S(1), N(2), O(2), and N(3) atoms comprising the square plane are −0.016(4), 0.093(10), −0.067(8), and 0.094(10) Å, respectively and the vanadium atom lies 0.639 Å out of this plane toward the apical oxo atom O(1). The trans O(2)−V−S(1) and N(2)−V−N(3) angles are 142.0(3)° [141.7(3)° for the second molecule] and 148.9-

(32) *TeXsan Software for Single-Crystal Structure Analysis*, version 1.7; Molecular Structure Corp.: 3200A Research Forest Drive, The Woodlands, TX 77381, 1997.

(33) Félix, O.; Hosseini, M. W.; De Cian, A.; Fischer, J. *Angew. Chem., Int. Ed. Engl.* **1997**, *36*, 102.

(34) Ghosh, S.; Nanda, K. K.; Addison, A. W.; Butcher, R. J. *Inorg. Chem.* **2002**, *41*, 2243.

(35) Li, X.; Lah, M. S.; Pecoraro, V. L. *Inorg. Chem.* **1988**, *27*, 4657.

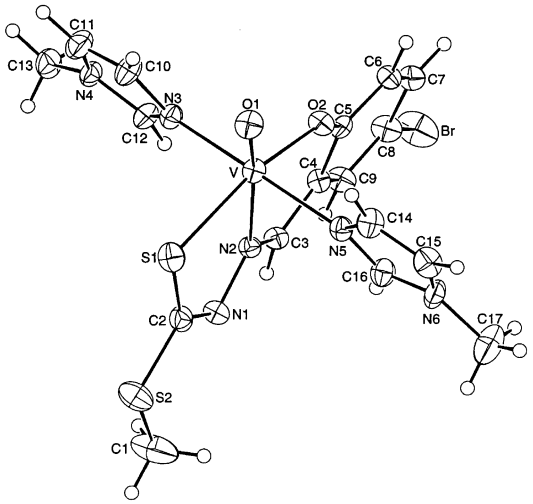

Figure 2. ORTEP diagram of $[VOL^3(N\text{-MeIm})_2]$ (**1b**) with 30% thermal probability ellipsoids showing the atomic numbering scheme.

Table 2. Selected Bond Lengths (Å) and Angles (deg) for Complexes **1a**,**b**

	1a	1b
	Bond Lengths	
V−O(1)	1.599(8), 1.609(8)	1.603(3)
V−S(1)	2.359(4), 2.348(4)	2.423(2)
V−O(2)	1.896(7), 1.911(7)	1.938(3)
V−N(2)	2.056(10), 2.073(9)	2.238(4)
V−N(3)	2.071(10), 2.063(9)	2.114(4)
V−N(5)		2.119(4)
	Bond Angles	
O(2)−V−S(1)	142.0(3), 141.7(3)	159.79(9)
N(2)−V−N(3)	148.9(4), 149.9(4)	88.2(1)
O(1)−V−O(2)	108.5(4), 108.5(4)	106.2(1)
O(1)−V−N(2)	104.6(4), 104.7(4)	170.6(2)
O(1)−V−S(1)	109.3(4), 109.7(4)	94.0(1)
O(1)−V−N(3)	106.2(4), 105.2(4)	92.9(2)
O(2)−V−N(2)	87.3(4), 87.2(3)	83.2(1)
N(2)−V−S(1)	79.3(3), 80.0(3)	76.6(1)
S(1)−V−N(3)	86.7(3), 87.7(3)	89.8(1)
N(3)−V−O(2)	86.9(4), 85.6(3)	89.7(1)
N(5)−V−N(3)		173.8(2)
N(5)−V−O(1)		93.0(2)
N(5)−V−N(2)		86.2(1)
N(5)−V−S(1)		91.6(1)
N(5)−V−O(2)		86.9(1)

(4)° [149.9(4)°], respectively. The V═O_t distance 1.599(8) Å [1.609(8) Å] is not exceptional.[36]

Compound **1b** crystallizes in a monoclinic space group $P2_1/c$ with four molecules accommodated in the unit cell. It has an octahedral geometry (Figure 2). Two terminal donor atoms O(2) and S(1) from the tridentate ligand along with N(3) and N(5) atoms from the monodentate *N*-methylimidazole molecules define the equatorial plane and lie −0.153(3), −0.116(2), 0.134(4), and 0.135(4) Å, respectively, out of the least-squares plane through them. The terminal oxo atom O(1) along with N(2) from the tridentate ligand occupy the axial positions and form an O(1)−V−N(2) angle of 170.6(2)°. The V atom is displaced from the mean equatorial plane toward the vanadyl oxygen atom (O(1)) by 0.241(1)

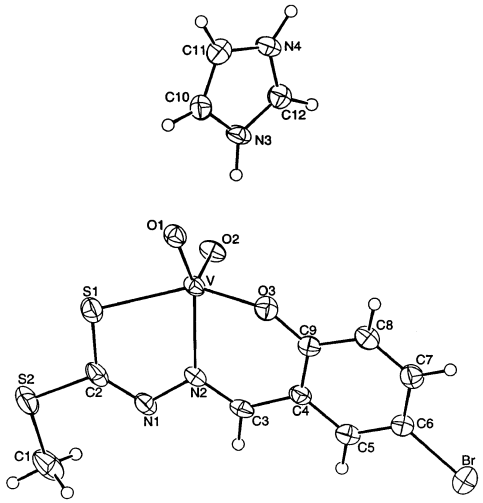

Figure 3. Molecular structure and atom-numbering scheme for the monomeric unit of $[VO_2L^3(ImH)]_\infty$ (**2a**) with thermal ellipsoids drawn at the 30% probability level.

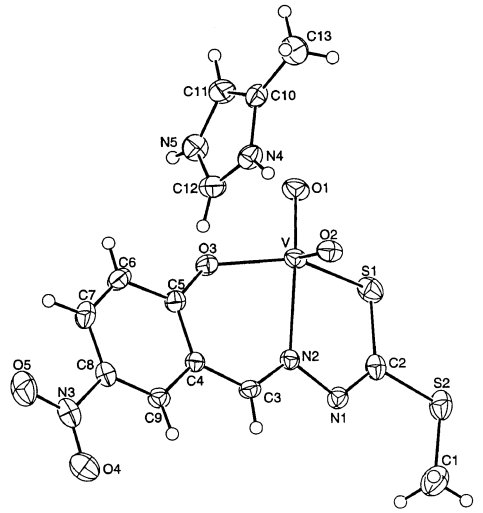

Figure 4. Molecular structure and atom-numbering scheme for the monomeric unit of $[VO_2L^2(4\text{-MeImH})]_\infty$ (**2d**) with thermal ellipsoids drawn at the 30% probability level.

Å. Of the three V−N distances in this molecule, the V−N(2) bond length (2.238(4) Å) has undergone a modest elongation due to trans labilizing influence of the terminal oxo group as observed in other oxovanadium complexes.[37] While N(5)−V−N(3) trans angle 173.8(2)° is close to the one required for an ideal square plane, some distortion is manifested in the O(2)−V−S(1) angle of 159.79(9)°, due to the restricted bite angle of the tridentate ligand.

The molecular structures of **2a**,**d** are shown in Figures 3 and 4, respectively. Important interatomic parameters are listed in Table 3. Strong hydrogen bonds link the imidazolium cations and LVO_2^- anions in both structures into zigzag chains, along the crystal screw axis in **2a** (Figure 5) and along the *c* glide direction in **2d** (Figure 6).

In each case, the vanadium(V) centers exist in a distorted square pyramidal geometry (Figures 3 and 4), with four basal

(36) (a) Vlahos, A. T.; Tolis, E. I.; Raptopoulou, C. P.; Tsohos, A.; Sigalas, M. P.; Terzis, A.; Kabanos, T. A. *Inorg. Chem.* **2000**, *39*, 2977. (b) Tsaramyrsi, M.; Kaliva, M.; Salifoglou, A.; Raptopoulou, C. P.; Terzis, A.; Tangoulis, V.; Giapintzakis, J. *Inorg. Chem.* **2001**, *40*, 5772.

(37) (a) Vergopoulos, V.; Priebsch, W.; Fritzsche, M.; Rehder, D. *Inorg. Chem.* **1993**, *32*, 1844. (b) Nakajima, K.; Kojima, M.; Toriumi, K.; Saito, K.; Fujita. J. *Bull. Chem. Soc. Jpn.* **1989**, *62*, 760.

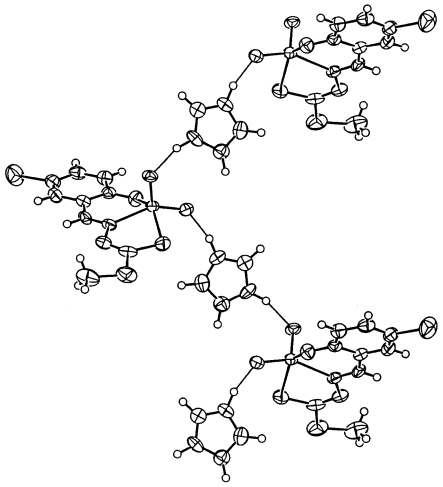

Figure 5. Extended chain structure of $[VO_2L^3(ImH)]_\infty$ (**2a**) due to hydrogen bonding along the crystal screw axis.

Table 3. Selected Bond Lengths (Å) and Angles (deg) for the Complexes **2a,d**

				2a		**2d**	
				Bond Lengths			
				V−S(1)		2.364(2)	2.342(1)
				V−O(1)		1.643(3)	1.666(2)
				V−O(2)		1.619(3)	1.604(2)
				V−O(3)		1.888(4)	1.902(2)
				V−N(2)		2.174(4)	2.176(2)
				Bond Angles			
				S(1)−V−O(1)		87.2(1)	87.98(8)
				S(1)−V−O(2)		106.4(1)	107.97(8)
				S(1)−V−O(3)		143.4(1)	139.72(7)
				S(1)−V−N(2)		76.5(1)	77.45(6)
				O(1)−V−O(2)		107.2(2)	107.3(1)
				O(1)−V−O(3)		96.9(2)	97.94(9)
				O(1)−V−N(2)		151.4(2)	156.9(1)
				O(2)−V−O(3)		107.0(2)	108.1(1)
				O(2)−V−N(2)		99.9(2)	94.38(9)
				O(3)−V−N(2)		83.4(2)	82.50(8)
				Hydrogen Bond Geometry			
	A	H	B	A···B	A−H	H···B	A−H···B
2a	N(3)	H(8)	O(2)	2.743(5)	0.9 5	1.82	162.7
	N(4)	H(9)	O(1)	2.709(5)	0.9 5	1.78	164.1
2d	N(4)	H(11)	O(1)	2.744(3)	0.9 3(4)	1.83(4)	168(4)
	N(5)	H(9)	O(1)	2.931(4)	0.8 1(4)	2.13(4)	166(4)

positions being occupied by the donors S(1), N(2), and O(3) from the coordinated tridentate ligands and one of the terminal oxo groups O(1). The axial site is taken up by the remaining oxo atom O(2) of the VO_2 core. In **2a**, O(2) forms angles in the range 99.9(2)−107.2(2)° with the basal plane (corresponding angles for **2d** vary between 94.38(9) and 108.1(1)°). The trans angles O(1)−V−N(2) 151.4(2)° [156.9(1)°] and S(1)−V−O(3) 143.4(1)° [139.72(7)°] are reasonably compressed, and the central vanadium atom is shifted by 0.541(1) Å [0.558(1) Å] from the basal plane toward the apical oxygen atom.

An interesting structural feature of these molecules is the presence of a bridging LVO_2^- unit which behaves like an inorganic analogue of a bridging carboxylate group.[38] While in **2a** the individual terminal oxo atoms of the $L^3VO_2^-$ units

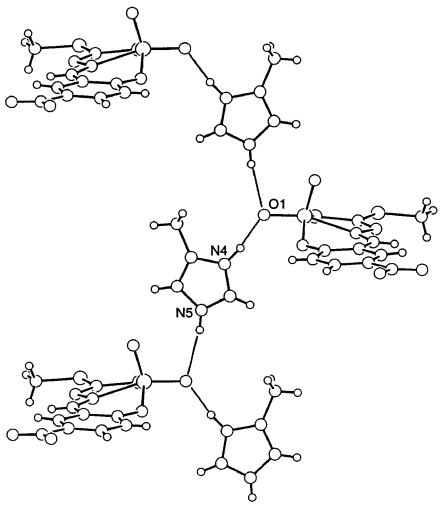

Figure 6. Extended chain structure of $[VO_2L^2(4\text{-MeImH})]_\infty$ (**2d**) due to hydrogen bonding along the *c*-glide plane.

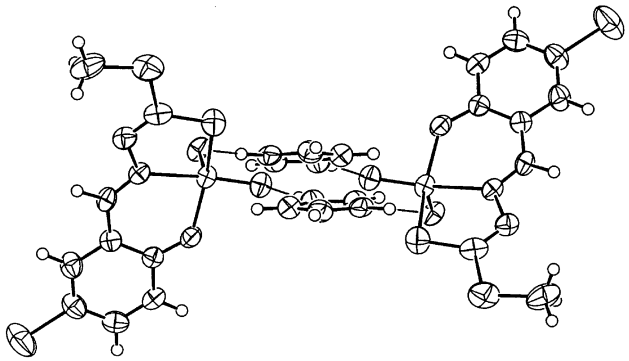

Figure 7. Hydrogen-bonded chain of $[VO_2L^3(ImH)]_\infty$ (**2a**) projected down the crystal screw axis, showing the nearly eclipsed imidazole rings.

are symmetrically attached to NH protons of the two neighboring imidazolium moieties (Figure 5), the corresponding mode of attachment of the $L^2VO_2^-$ units in **2d** is, however, asymmetric and takes place through the participation of a single terminal oxo group (the equatorial one), keeping the other free (Figure 6). The presence of a methyl group in the imidazole moiety seems to influence this asymmetric binding in **2d**. In **2a**, the two terminal oxo atoms attached to the NH protons of an imidazolium moiety are not exactly the same. While one of these is an apical oxo atom, the other happens to be an equatorial one coming from the immediately neighboring vanadium center. Since in an LVO_2^- unit these two oxo atoms are nearly orthogonal (O−V−O angle being 107° (Table 3)), that allows the neighboring imidazole moieties to nearly eclipse one another when viewed down the crystal screw axis (Figure 7).

Details of the hydrogen bond geometry in **2a**,**d** are also shown in Table 3.

Magnetism and EPR. Oxovanadium(IV) complexes **1a**−**c** are magnetically straightforward. At room temperature (298 K) the observed values of moments 1.69−1.71 μ_B (Table 4) are as expected for a simple $S = 1/2$ paramagnet with d_{xy}-based ground state.[39]

(38) Giacomelli, A.; Floriani, C.; De Souza Duarte, A. O.; Chiesi-Villa, A.; Guastini, C. *Inorg. Chem.* **1982**, *21*, 3310.

(39) Collison, D.; Gahan, B.; Garner, C. D.; Mabbs, F. E. *J. Chem. Soc., Dalton Trans.* **1980**, 667.

Table 4. Magnetic Moments and the Spin-Hamiltonian Parameters for the Vanadium(IV) Complexes (**1a**−**c**) and the Photoreduced Products (**2A**,**D**)

	μ_{eff}[a]	$\langle g\rangle$[b]	$g_{\|}$[c]	$g_{\perp}$[c]	$10^4\langle A\rangle$,[b] cm^{-1}	$10^4A_{\|}$[c] cm^{-1}	$10^4A_{\perp}$[c] cm^{-1}
1a	1.69	1.978	1.959	1.988	88	158	54
1b	1.71	1.988	1.972	1.995	51	103	32
1c	1.70	1.989	1.974	1.998	52	105	32
2A		1.945			45		
2D		1.961			46		

[a] Measured at room temperature with powdered polycrystalline samples. [b] From room-temperature spectra in CH_2Cl_2/toluene (1:1 v/v) solution (for **1a**−**c**) and in CH_3CN (for **2A**,**D**). [c] From frozen solution (77 K) spectra.

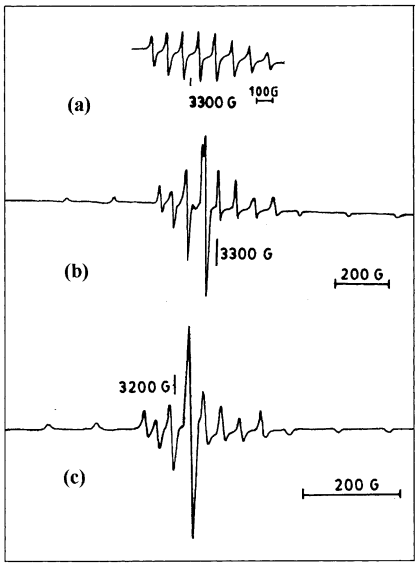

Figure 8. Solution (CH_2Cl_2/toluene, 1:1 v/v) EPR spectra (X-band) of (a) [VOL^3(BzIm)]·0.5CH_3CN (**1a**) at room temperature (298 K), (b) **1a** in frozen solution (77 K), and (c) [VOL^2(*N*-MeIm)$_2$] (**1c**) in frozen solution (77 K).

EPR spectra of the oxovanadium(IV) complexes look essentially identical. Spectra for **1a** measured both in the fluid (CH_2Cl_2/toluene, 1:1 v/v) as well as in the frozen solution (77 K) are shown in Figure 8. At room temperature, the spectrum (Figure 8a) shows typical eight-line pattern [$\langle g\rangle = 1.978$ and $\langle A\rangle = 88 \times 10^{-4}$ cm^{-1} (Table 4)], characteristic of an unpaired electron being coupled to the vanadium nuclear spin (^{51}V, 99.76 atom %, $I = 7/2$). In the frozen solution, however, the spectrum displays well-resolved axial anisotropy with two sets of eight-line patterns. Corresponding spin-Hamiltonian parameters ($g_{\|}$, 1.959; $A_{\|}$, 158×10^{-4} cm^{-1}; $g_{\perp}$, 1.988; $A_{\perp}$, 54×10^{-4} cm^{-1}) are typical of square pyramidal oxovanadium(IV) complexes under comparable sulfur-containing donor environments.[40,41] Of particular interests are the subtle but interesting differences in the EPR parameters of **1a**−**c**, summarized in Table 4. For the octahedral complexes (**1b**,**c**), the anisotropic hyperfine parameters have significantly lower values ($A_{\|}$, 105×10^{-4} cm^{-1}; $A_{\perp}$, 32×10^{-4} cm^{-1}) compared to the corresponding values obtained with the square pyramidal complex **1a**. The EPR spectrum (in frozen solution, 77 K) of a representative octahedral complex (**1c**) is displayed in Figure 8c. Such lower *A* values are rarely observed for six-coordinated vanadium(IV) complexes and have been explained as due to delocalization of the odd electron over the sulfur-containing ligand environment.[42]

Table 5. Summary of Electronic Spectroscopic Data for the Complexes in Solution

	solvent	λ_{max}, nm (ϵ, mol^{-1} cm^2)
1a	CH_3CN	721 (220), 523 (190), 400 (10 500), 343 (7400), 299 (15 500), 222 (37 300)
	CH_2Cl_2	692 (100), 522 (145), 403 (12 800), 346 (10 400), 301 (18 200)
1b	CH_3CN	707 (30), 517 (90), 400 (10 700), 340 (7500), 300 (12 500), 218 (34 500)
	CH_2Cl_2	694 (30), 520 (100), 403 (15 900), 345 (11 050), 298 (18 700)
1c	CH_3CN	706 (30), 517 (210), 382 (17 000), 336 (14 400), 306 (25 800), 215 (27 700)
2a	CH_3CN	400 (8100), 283 (20 800), 232 (27 500)
	acetone	403 (8800)
	methanol	386 (8100), 300 (27 300), 228 (34 900)
2b	CH_3CN	382 (14 800), 311 (24 100), 229 (23 500)
	acetone	381 (11 200)
	methanol	365 (sh), 314 (29 300), 227 (21 000)
2c	CH_3CN	401 (8500), 285 (21 200), 233 (28 200)
	acetone	401 (9900)
2d	CH_3CN	382 (17 200), 311 (28 100), 222 (31 000)
	acetone	379 (13 200)
	methanol	370 (sh), 308 (24 250), 223 (24 050)

Electronic Spectra. The electronic absorption spectra of the complexes are summarized in Table 5. All the vanadium(V) complexes (**2a**−**d**) display an intense to medium-intensity electronic spectral band in the near-UV region. In acetonitrile and acetone, this band appears at ca. 400 nm in **2a**,**c** and blue-shifted to ca. 380 nm in **2b**,**d** when the *para* substituent in the tridentate ligand framework is changed from bromo to nitro group. We believe this band is originating from ligand-to-metal charge-transfer (LMCT), arising from the phenolate oxygen to an empty d-orbital of the vanadium(V) center. Of particular interest here is the position of this LMCT band in methanol which suffers a major blue-shift compared to what has been observed in a weakly coordinating solvent, viz. acetonitrile or acetone (Table 5). We believe this spectral change is originating from the participation of methanol in coordination to vanadium as corroborated also by ^{1}H NMR experiment (see later).

The oxovanadium(IV) complexes (**1a**−**c**) have closely similar electronic spectra in acetonitrile and dichloromethane solution. Like the vanadium(V) complexes (**2a**−**d**), these spectra show an intense LMCT [PhO → V(dπ)] band in the 382−403 nm range. In addition, these complexes also display two ligand field absorptions of moderate intensities (ϵ, 30−220 mol^{-1} cm^2) in the 692−721 and 517−523 nm range, corresponding to the transitions $d_{xy} \rightarrow d_{xz}$, d_{yz} and $d_{xy} \rightarrow d_{x^2-y^2}$, respectively, as expected from an idealized square pyramidal (C_{4v}) oxovanadium(IV) species.[43] For the octahedral complexes **1b**,**c**, the presence of a sixth donor ligand, trans to

(40) Dickson, F. E.; Kunesh, C. J.; McGinnis, E. L.; Petrakis, L. *Anal. Chem.* **1972**, *44*, 978.
(41) Klich, P. R.; Daniher, A. T.; Challen, P. R.; McConville, D. D.; Youngs, W. J. *Inorg. Chem.* **1996**, *35*, 347.
(42) Davidson, A.; Edelstein, N.; Holm, R. H.; Maki, A. H. *J. Am. Chem. Soc.* **1964**, *86*, 2799.
(43) Hahn, C. W.; Rasmussen, P. G.; Bayón, J. C. *Inorg. Chem.* **1992**, *31*, 1963.

Table 6. ^{1}H NMR Spectral Data (δ, ppm)[a] for the Vanadium(V) Complexes in Different Solvents at Room Temperature

2a			**2c**		**2d** in		
methanol-d_4	acetone-d_6	acetonitrile-d_3	methanol-d_4	acetonitrile-d_3	acetonitrile-d_3	integration	assgnt
8.84, 8.77 s	8.95 s	8.88 s	8.84, 8.77 s	8.90 s	9.03 s	1H	H_4
8.26 s	8.86 s	8.51 s	8.34 s	8.43 s	8.54 s	1H	H_6
7.63, 7.73 s	7.69 s	7.69 s	7.63, 7.72 s	7.71 s	8.24 s	1H	H_3
7.40 (7.8), 7.53 (8.8) d	7.37 (8.8) d	7.50 (6.0) d	7.40 (8.7), 7.52 (8.8) d	7.49 s	8.16 s	1H	H_2
7.24 s	7.63 s	7.41 s	7.02 s	7.13 s	7.05 s	2H/1H[b]	H_9, H_8
6.82 (8.8), 6.78 (8.8) d	6.72 (9.0) d	6.86 (9.0) d	6.81 (8.5), 6.78 (8.9) d	6.87 (9.0) d	6.99 (12.0) d	1H	H_1
2.50, 2.48 s	2.42 s	2.57 s	2.48, 2.50 s	2.54 s	2.53 s	3H	H_5
			2.22 s	2.33 s	1.27 s	3H	H_{11}

[a] Chemical shift (δ) relative to internal TMS. Proton labels are as in Figure 9: s, singlet; d, doublet. Values in the parentheses represent coupling constants (J in Hz). [b] Complexes **2c**,**d** have a methyl substitution in the imidazole ring.

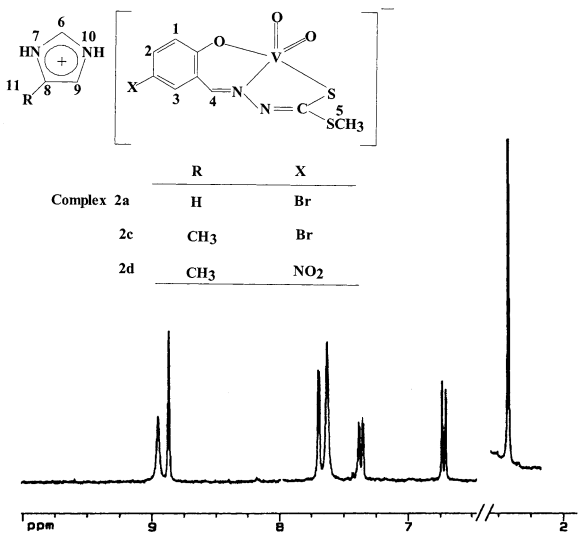

Figure 9. 300 MHz ^{1}H NMR spectrum of $[VO_2L^3(ImH)]_\infty$ (**2a**) in acetone-d_6 solution at 25 °C.

the terminal V═O bond, has a direct influence so that the d−d transitions here are systematically blue-shifted compared to the corresponding band positions obtained with the square-pyramidal complex **1a** (Table 5).[26]

All the remaining bands in the UV region are due to intraligand transitions.

^{1}H NMR Spectroscopy. ^{1}H NMR spectra of the vanadium(V) complexes, taken in a number of solvents, are summarized in Table 6. Free tridentate ligands have two broad resonances at ca. 10.9 and 10.5 ppm region due to phenolic OH and NH protons, respectively. These signals are absent in the spectra of the complexes indicating that the tridentate ligands are dianionic. The spectrum of **2a** in acetone-d_6 (Figure 9) involves two singlets at 8.86 and 7.63 ppm due to imidazolium ring CH protons. The NH protons of the imidazolium ring are not clearly visible in the spectrum. Two other singlets at 8.95 and 2.42 ppm are characteristics of the azomethyne and SCH_3 protons, respectively. Remaining peaks in the aromatic region appear with expected multiplicities as outlined in Table 6

The spectrum of **2a** in methanol-d_4 looks a little more complicated as shown in Figure 10. A careful scrutiny of this figure reveals that the signals due to protons belonging to the tridentate ligand (L^3) appear in pair with expected multiplicities while those due to imidazolium ring CH protons (at 8.26 and 7.24 ppm) appear only once. We believe

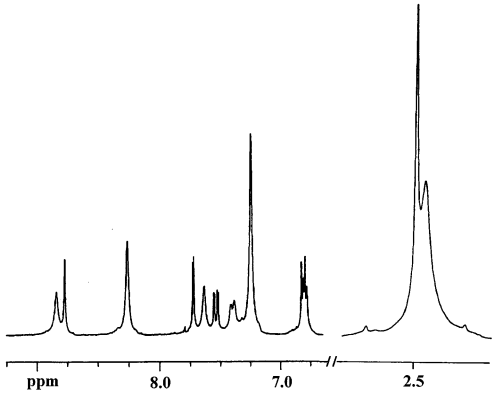

Figure 10. 300 MHz ^{1}H NMR spectrum of $[VO_2L^3(ImH)]_\infty$ (**2a**) in methanol-d_4 solution at 25 °C showing features due to solvation equilibrium.

this is due to an equilibrium (eq 1) involving a weak coordination of the solvent methanol as established also by electronic spectral studies (vide supra). In fact, the corresponding isoelectronic molybdenum(VI) compound $[MoO_2L^1(CH_3OH)]$ has been isolated and crystallographically characterized.[44]

$$[VO_2(L^3)(ImH)] + CH_3OH \rightleftharpoons [VO_2(L^3)(CH_3OH)](ImH) \quad (1)$$

In dry acetonitrile, fresh yellow solutions of **2a**−**d** gradually turn green when exposed to visible light. Progress of such photochemical reaction has been monitored by dynamic ^{1}H NMR experiments. It appears that all the prominent spectral features except those due to imidazole ring CH protons have undergone gradual line-broadening with concomitant loss in spectral resolution as the exposure time is increased. Results indicate the formation of paramagnetic species in solution as a probable product by the reduction of VO_2L^- species through a photochemical pathway as confirmed by control experiments.[22] Similar photo-induced reduction also occur in other aprotic donor solvents such as DMF and DMSO.

Characterization of the Photoreduced Product. Despite our repeated attempts, we remained unsuccessful in isolating the green photoreduced products (**2A**−**D**) in the solid state. In solution, however, the photoreduced products are all EPR active unlike their *cis*-dioxovanadium(V) precursors (**2a**−

(44) Dutta, S. K.; McConville, D. B.; Youngs, W. J.; Chaudhury, M. *Inorg. Chem.* **1997**, *36*, 2517.

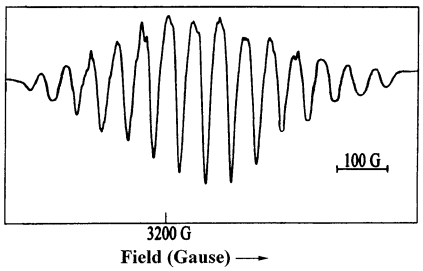

Figure 11. X-band EPR spectrum of a photoreduced solution of $[VO_2L^3(ImH)]_\infty$ (**2a**) in dry acetonitrile at room temperature after 12 h exposure to visible light.

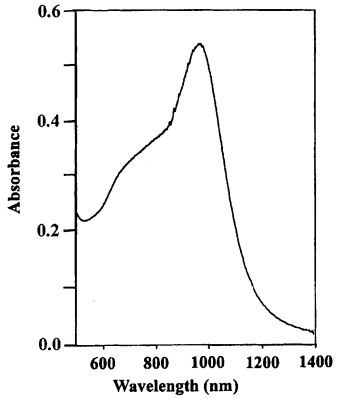

Figure 12. Vis−NIR electronic absorption spectrum of a photoreduced solution of **2a** (~1.41 × 10^{-3} M) in acetonitrile after 12 h exposure to visible light.

d). The spectrum of a representative product **2A** (corresponding precursor complex being **2a**) is shown in Figure 11 which reveals a 15-line feature ($\langle g \rangle = 1.945$) at room temperature with asymmetric distortions. The product appears to have a coupled divanadium center with an odd interacting electron generating the 15-line structure with $\langle A \rangle = 45 \times 10^{-4}$ cm^{-1}, which is almost half as much as that of a localized spectrum ($\langle A \rangle_8 = 89 \times 10^{-4}$ cm^{-1}) reported earlier[20] for a μ-oxo divanadium(IV/V) product with related ligand. This observation, none the less, speaks in favor of a mutually interacting divanadium(IV/V) species to be the product of this photoinduced reduction.[45] The observed asymmetry in the spectrum (Figure 11) probably has its origin in a solvent-dependent equilibrium process involving two magnetically inequivalent structural forms of the divanadium(IV/V) compound as reported elsewhere[20] for a related system.

Freshly prepared yellow solutions of **2a**−**d** in CH_3CN are all optically transparent in the visible/near-IR region (Table 5). The green solutions of the photoreduced products, on the other hand, absorb strongly in the 1300−500 nm region. The spectrum of **2A** in the relevant region is shown in Figure 12, as a representative example. It involves an absorption maximum of moderate intensity at 982 nm followed by a low-intensity shoulder, centered around 726 nm, the absorption ratio, A_{982}/A_{726} being close to 1.50 after a 12 h exposure time. The shape and position of this near-IR band is quite similar to that of an intervalence charge-transfer band of an authentic mixed-oxidation (μ-oxo)divanadium(IV/V) complex previously reported by us.[20] The absorption in the visible region appears due to ligand-field transition(s), localized on the oxovanadium(IV) center of this mixed-oxidation divanadium(IV/V) species.

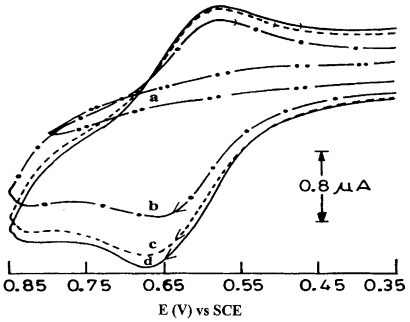

Figure 13. Traces of cyclic voltammograms recorded with a solution of **2d** in dry acetonitrile during the progress of photoreduction: (a) fresh solution; (b) after 3 h; (c) after 6 h; (d) after 12 h exposure to visible light (potentials vs SCE, 0.1 M TEAP at a glassy carbon working electrode, scan rate 50 mV s^{-1}).

Another interesting feature of the photoreduced products is their electrochemical response as studied by cyclic voltammetry. Although the precursor complexes (**2a**−**d**) are all electrochemically inactive in the potential range −1.0 to +1.0 V vs SCE, their photoreduced counterparts display the development of an oxidation process as revealed from the voltammogram of **2D** (Figure 13) shown as a representative example, the corresponding precursor complex being **2d**. On the basis of comparison with the ferrocenium/ferrocene couple ($\Delta E_p = 80$ mV, $i_{pc}/i_{pa} = 1.0$ at 50 mV s^{-1}), this oxidation process ($\Delta E_p = 90$ mV, $i_{pa}/i_{pc} = 1.1$ at 50 mV s^{-1}) may be described as nearly reversible[46] involving one-electron transfer (eq 2) as reported earlier with a related mixed-oxidation (μ-oxo)divanadium(IV/V) compound.[19] Because of a strong electron-withdrawing nitro group substitution in the ligand structure, this oxidation is more difficult in **2D** ($E_{1/2} = 0.63$ V) relative to that with the bromo derivative **2A** ($E_{1/2} = 0.50$ V, potentials are vs SCE).

$$[LOV^V{-}O{-}V^{IV}OL]^- \overset{-e^-}{\rightleftharpoons} [LOV^V{-}O{-}V^VOL]^0 \quad (2)$$

Results of EPR, electrochemical, and electronic spectral studies seem to support the generation of a (μ-oxo)-divanadium(IV/V) species during the photochemical transformation of **2a**−**d** in dry CH_3CN solution.

Concluding Remarks

Reactions of $[VO(acac)_2]$ with the tridentate ONS ligands (H_2L^2 and H_2L^3) in aqueous acetonitrile medium generate oxovanadium(IV) (**1a**−**c**) and -(V) (**2a**−**d**) complexes in the presence of various imidazole derivatives as coligands. With imidazole and 4-methylimidazole, the products obtained are *cis*-dioxovanadium(V) complexes $[VO_2L(R'\text{-ImH})]$ (**2a**−**d**). In the solid state, these complexes have interesting zigzag chain structures as revealed from the X-ray crystallographic investigation of **2a**,**d**, involving an alternating array of LVO_2^-

(45) Slichter, C. P. *Phys. Rev.* **1955**, *99*, 478.

(46) Brown, E. R.; Large, R. F. Electrochemical Methods. In *Physical Methods in Chemistry*; Weissberger, A., Rossiter, B., Eds.; Wiley-Interscience: New York, 1971; Part IIA, Chapter VI.

species and the corresponding imidazolium counterions, held together by Coulombic interactions and strong hydrogen bonding. These LVO_2^- species are stable in water and methanol as appeared from ^1H NMR and electronic spectral studies. But in aprotic solvents such as CH_3CN, DMF, or DMSO, they undergo proton-coupled photoinduced reduction (eqs 3 and 4) through the intermediate formation of hydroxo species LVO(OH).[35,47,48] The reduced $LV^{IV}O$ species, thus formed, reacts with excess LVO_2^- units to generate the mixed-oxidation divanadium(IV/V) products **2A**−**D** (eq 5).[49] Structurally characterized mixed-oxidation poly(oxo)vanadate(IV/V) compounds prepared by photoinduced reduction have been reported recently in the literature.[50]

$$LV^{V}O_2^- + H^+ \rightleftharpoons LV^{V}O(OH) \quad (3)$$

$$LV^{V}O(OH) + H^+ + e^- \overset{h\nu}{\rightleftharpoons} LV^{IV}O + H_2O \quad (4)$$

$$LV^{IV}O + LV^{V}O_2^- \rightleftharpoons [LV^{IV}O-(\mu\text{-}O)-OV^{V}L]^- \quad (5)$$

When imidazole is replaced by benzimidazole or *N*-methylimidazole, the products are mononuclear oxovanadium(IV) complexes (**1a**−**c**) with interesting variations in structure. In solution, **1a** has a tendency to undergo aerial oxidation at a much slower rate, while **1b**,**c** are resistant to similar aerial oxidation under comparable condition. We believe the strength of the imidazole bases plays a crucial role here in controlling the rate of aerial oxidation of the $LV^{IV}O$ precursors. Stronger bases such as 4-methylimidazole (basic pK_a, 7.61) and imidazole (basic pK_a, 6.95) are efficient enough to stabilize the oxidized anionic *cis*-VO_2 species by forming salts of their symmetrical mesomeric cations.[51] Benzimidazole (basic pK_a, 5.5) and *N*-methylimidazole, on the other hand, have a little or no capability to generate the protonated symmetrical cation needed for the stability of the oxidized *cis*-dioxovanadium(V) product.

Acknowledgment. Financial support received from the Council of Scientific and Industrial Research, New Delhi, is gratefully acknowledged. We thank Professor K. Nag for many useful discussions.

Supporting Information Available: X-ray crystallographic files in CIF format for compounds **1a**,**b** and **2a**,**d**. This material is available free of charge via the Internet at http://pubs.acs.org.

IC020438V

(47) Root, C. A.; Hoeschele, J. D.; Cornman, C. R.; Kampf, J. W.; Pecoraro, V. L. *Inorg. Chem.* **1993**, *32*, 3855.
(48) Asgedom, G.; Sreedhara, A.; Kivikoski, J.; Kolehmainen, E.; Rao, C. P. *J. Chem. Soc., Dalton Trans.* **1996**, 93.
(49) Nishizawa, M.; Hirotsu, K.; Ooi, S.; Saito, K. *J. Chem. Soc., Chem. Commun.* **1979**, 707.
(50) Yamase, T.; Suzuki, M.; Ohtaka, K. *J. Chem. Soc., Dalton Trans.* **1997**, 2463.
(51) *Comprehensive Organic Chemistry*; *Vol. 4*, *Heterocyclic Chemistry*; Sammes, P. G., Ed.; Pergamon Press: Oxford, England, 1979; p 364.